Hindawi
Mobile Information Systems
Volume 2022, Article ID 4186973, 12 pages
https://doi.org/10.1155/2022/4186973

*Research Article*

# Propulsion Energy Minimization for Fixed-Wing-UAV-Assisted Full-Duplex Mobile Relaying via Hybrid Trajectory Design

**Senyi Shi**,[1] **Xiaodong Ji**,[1] **Tao Wang**,[1] **Chong Qian**,[2] **and Chenhao Huang**[3]

[1]*School of Information Science and Technology, Nantong University, Nantong, Jiangsu 226019, China*
[2]*Wujiang Branch of China Telecom Group Co, Suzhou, Jiangsu 215200, China*
[3]*Gaoyou Branch of China Telecom Group Co, Yangzhou 225600, China*

Correspondence should be addressed to Xiaodong Ji; jxd@ntu.edu.cn

Received 29 August 2022; Accepted 27 October 2022; Published 14 November 2022

Academic Editor: Jose F. Monserrat



This paper solved a propulsion energy minimization problem subject to a total data-bit constraint of an unmanned aerial vehicle (UAV)-enabled full-duplex mobile relaying system, where a fixed-wing UAV is dispatched as a full-duplex mobile relay to assist data transfer from a source to a destination. Here, three trajectory flying modes are used, namely, the UAV first flies along a circular path above the source, next flies to the destination along a straight line, and finally flies along a circular path above the destination until all the data-bits have been transferred. Since the propulsion energy minimization problem is a nonconvex mixed integer programming problem, its closed-form solution is not tractable, and hence, it is transformed to three subproblems so as to simplify its solution. After solving the three subproblems, an iterative algorithm is proposed to achieve a suboptimal solution to the propulsion energy minimization problem, leading to a new hybrid circular/straight trajectory (HCST) design. Computer simulations are conducted to validate the effectiveness of the proposed HCST design. It is shown that the proposed HCST design performs well in terms of energy saving for the long distance and big data communication cases compared with the straight or circular flight trajectory design.

## 1. Introduction

The use of unmanned aerial vehicles (UAVs) for assisting wireless communications has attracted increasing interest recently [1, 2]. Compared to the traditional terrestrial communications, UAV-assisted communications are more cost-effective, flexible, and swift for deployment due to the high mobility of UAVs and the possibility of providing on-demand services. In addition, UAV-ground communications are more likely to have line-of-sight (LoS) channels which offer higher capacity than that provided by terrestrial links. Thus, UAVs shall play an extremely important role in wireless communication applications such as temporary traffic offloading for cellular base stations [3, 4], cooperative communications for mobile relaying [5–8], and information dissemination and data collection for Internet of Things [9, 10].

In this paper, we considered a full-duplex mobile relaying system consisting of a fixed-wing UAV, a source, and a destination. The source would like to transfer data to the destination assisted by the fixed-wing UAV which acts as a full-duplex decode-and-forward (DF) relay. The UAV relay has three trajectory flying modes, namely, the UAV first flies along a circular path above the source, next flies to the destination along a straight line, and finally flies along a circular path above the destination until all the data-bits have been transferred. It is noted in [11] that the communication-related power of a UAV is usually much smaller than its propulsion power. Therefore, the main goal of this paper is to minimize the total propulsion energy of the UAV. We formulate the trajectory design as a nonconvex mixed integer programming problem. To solve the problem, it is divided into a few subproblems, by solving which a suboptimal solution is acquired. Then, an iterative algorithm is proposed to obtain a hybrid circular/straight trajectory (HCST) design which can approach to the optimal trajectory and minimize the total propulsion energy accordingly.

The rest of this paper is organized as follows: Section 2 describes the related works in literature. Section 3 introduces the system model under investigation and formulates a general optimization problem corresponding to the UAV's propulsion energy minimization. By dividing the optimization problem into three subproblems, the energy minimization problem is solved in Section 4, leading to a new HCST design. Computer simulations and performance comparisons are presented in Section 5. Section 6 concludes the paper.

## 2. Related Works

Currently, there are many works in the literature that concern the problem of maximizing information throughput or spectrum efficiency of UAV-assisted mobile relaying systems [12–16]. It is known that UAVs have limited on-board energy, and thus energy saving has been recognized as a more important factor for UAV communications. The authors of [17] investigated an energy-efficiency problem by optimizing the UAV's speed and load factors in a circular trajectory. In [18], collaboration schemes between multiple UAVs were investigated so as to extend the duration of communications. On this basis, a joint design of UAV-trajectories and the transmit power of the communication nodes were proposed with the aim of maximizing the end-to-end throughput. In [19], a power consumption trade-off between ground terminals and UAVs were derived for circular and straight trajectories, respectively. The authors of [11] developed a load-carry-and-delivery scheme for a full-duplex UAV relaying network with the aim of enhancing the energy efficiency of the network. In [20], a rotary-wing UAV was used to communicate with multiple ground nodes, and an efficient algorithm was proposed to optimize the hovering locations and duration, as well as the flying trajectory so as to minimize the system energy consumption. The authors of [21] investigated an energy-efficiency problem with the aim of maximizing the data-bits transferred per the UAV's propulsion energy via the trajectory design of the UAV. It should be noted that most of the existing works considered circular or straight trajectory design separately. The authors of [22] took a fuel-powered rotary-wing UAV relaying system into consideration and proposed a joint optimization method for power control of the communication terminals and the UAV's trajectory design so as to maximize the system energy efficiency. It is noted in [21] that there exists an upper bound of information throughput if a straight trajectory is adopted. It means that a straight trajectory is not suitable for the case where a huge amount of data need to be transferred. In case that a circular trajectory is employed, the system information throughput will be poor if the source and destination nodes are located far away [17]. In view of the shortcomings of circular and straight trajectories, this paper investigates an HCST design for propulsion energy minimization of the system.

## 3. System Model and Problem Description

Figure 1 gives the system model, where a UAV denoted by $R$ is dispatched as a mobile relay to assist data transfer from the source $S$ to the destination $D$. Suppose that $S$ and $D$ are located far away, and thus no direct link exists between $S$ and $D$ due to high path loss caused by long distance and/or obstacles. Moreover, it is assumed that $S$ would like to transfer a huge amount of data to $D$.

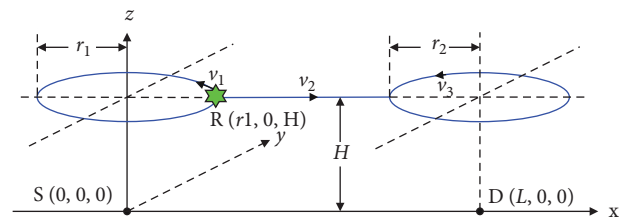


Figure 1: UAV-assisted mobile relaying system with hybrid circular/straight trajectory.

Without loss of generality, assume that the horizontal coordinates of $S$ and $D$ are $q_S = [0,0]^T$ and $q_D = [L,0]^T$, respectively, where $L$ is the distance between $S$ and $D$, and the UAV flies at a fixed altitude $H$ which corresponds to the minimum altitude required for terrain or building avoidance without frequent aircraft ascending or descending [11]. Denote by $T$ the mission time. Throughout the whole mission time, the UAV needs to collect $Q$ data-bits from $S$ and then forwards them to D. There exist three trajectory modes described as the following:

Mode 1: the UAV flies along a circular path with center at $(0,0,H)$ and radius $r_1$. Denote by $v_1$ and $T_1$ the UAV's speed and duration of mode 1, respectively.

Mode 2: the UAV flies from $(r_1,0,H)$ to $(L-r_2,0,H)$ along a straight line. Denote by $v_2$ and $T_2$ the UAV's speed and duration of mode 2, respectively.

Mode 3: the UAV flies along a circular path with center at $(L,0,H)$ and radius $r_2$. Denote by $v_3$ and $T_3$ the UAV's speed and duration of mode 3, respectively.

Suppose that the initial location of the UAV is $(r_1,0,H)$. First, the UAV flies $n$ laps according to mode 1. Then, the UAV flies along mode 2. Finally, the UAV flies according to mode 3 until $Q$ bits-data are completely transferred from $S$ to $D$. Here, the duration of each mode must satisfy

$$T_1 = \frac{2\pi r_1}{v_1} n,\ (n = 1,2,\cdots), T_2 = \frac{L - r_1 - r_2}{v_2}, T_3 \geq 0. \quad (1)$$

During the whole mission time, a full-duplex relaying fashion is employed, namely, the UAV collects data from $S$ and forwards them to $D$, simultaneously. Note that, for simplicity, the UAV's take-off and landing phases are ignored. It is worth-mentioning that the UAV's trajectory should change between different modes smoothly, and the UAV's speed cannot be switched instantly between $v_1$, $v_2$, and $v_3$. Since the total energy consumption of a UAV is quite large, the change of the UAV's kinetic energy between speeds $v_1$, $v_2$, and $v_3$, and the differences between the practical trajectory and the trajectory in Figure 1 can be omitted. Denote by $q(t) \in R^{2\times 1}$ the UAV's trajectory on the horizontal coordinate, where $0 \leq t \leq T$. Then, the time-varying distance between $S$ and $R$, and that between $R$ and $D$ can be, respectively, expressed as follows:

$$d_{\mathrm{SR}}(t) = \sqrt{H^2 + \|\mathrm{q}(t)\|^2}, \tag{2}$$

$$d_{\mathrm{RD}}(t) = \sqrt{H^2 + \left\|(L,0)^T - \mathrm{q}(t)\right\|^2}. \tag{3}$$

Here, it is assumed that $R$ is equipped with a data-buffer of sufficiently large size and the communication links from $R$ to $S$ and $D$ are dominated by LoS channels [12]. Moreover, the Doppler effect due to the UAV mobility is assumed to be perfectly compensated [12]. Then, the time-varying channel between $S$ and $R$ follows the free-space path loss model and can be written as follows:

$$h_{\mathrm{SR}}(t) = \beta_0 d_{\mathrm{SR}}^{-2}(t) = \frac{\beta_0}{H^2 + \|\mathrm{q}(t)\|^2}, \tag{4}$$

where $\beta_0$ denotes the channel power at the reference distance $d_0 = 1$ m.

Likewise, the time-varying channel between $R$ and $D$ can be expressed as follows:

$$h_{\mathrm{RD}}(t) = \beta_0 d_{\mathrm{RD}}^{-2}(t) = \frac{\beta_0}{H^2 + \left\|(L,0)^T - \mathrm{q}(t)\right\|^2}. \tag{5}$$

Assume that $R$ collects and forwards data using different frequency bands, and thus there is no loop-interference at the UAV [12]. Then, the corresponding signals received by $R$ and $D$ can be, respectively, written as follows:

$$y_{\mathrm{R}}(t) = \sqrt{P_{\mathrm{S}} h_{\mathrm{SR}}(t)}\, x_{\mathrm{S}}(t) + n_{\mathrm{R}}(t), \tag{6}$$

$$y_{\mathrm{D}}(t) = \sqrt{P_{\mathrm{R}} h_{\mathrm{RD}}(t)}\, x_{\mathrm{R}}(t) + n_{\mathrm{D}}(t). \tag{7}$$

In (6) and (7), $x_S(t)$ and $x_R(t)$ are the signals sent by $S$ and $R$; $P_S$ and $P_R$ are the transmit power from $S$ and $R$; $n_R(t)$ and $n_D(t)$ are the additive noises received by $R$ and $D$, respectively.

The data of size $Q_R(t)$ and $Q_D(t)$ received by $R$ and $D$ at time $t$ can be, respectively, expressed as follows [11]:

$$\begin{aligned} Q_{\mathrm{R}}(t) &= \int_0^t \log_2\left(1 + \frac{P_{\mathrm{S}} h_{\mathrm{SR}}(\tau)}{\sigma^2}\right)\mathrm{d}\tau \\ &= \int_0^t \log_2\left(1 + \frac{P_{\mathrm{S}}\gamma_0}{H^2 + \|\mathrm{q}(\tau)\|^2}\right)\mathrm{d}\tau, \end{aligned} \tag{8}$$

$$\begin{aligned} lptQ_{\mathrm{D}}(t) &= \int_0^t \log_2\left(1 + \frac{P_{\mathrm{R}} h_{\mathrm{RD}}(\tau)}{\sigma^2}\right)\mathrm{d}\tau \\ &= \int_0^t \log_2\left(1 + \frac{P_{\mathrm{R}}\gamma_0}{H^2 + \left\|(L,0)^{\mathrm{T}} - \mathrm{q}(\tau)\right\|^2}\right)\mathrm{d}\tau, \end{aligned} \tag{9}$$

where $\gamma_0 \triangleq \beta_0/\sigma^2$ and $\sigma^2$ denotes the noise power at $R$ and $D$. It is worth-mentioning that in the paper, data-bit is normalized by bandwidth, and thus its unit is bit/Hz. Unless otherwise specified, bit means bit/Hz in the paper. In order to ensure $Q$ bits-data transfer during mission time $T$, (10) must be satisfied.

$$Q_{\mathrm{R}}(T) \geq Q, Q_{\mathrm{D}}(T) \geq Q. \tag{10}$$

Moreover, the UAV can only forward data that has already been collected from $S$, and thus the following information-causality constraint must be satisfied [20].

$$Q_{\mathrm{D}}(t) \leq Q_{\mathrm{R}}(t), 0 \leq t \leq T. \tag{11}$$

It is well known that the total power consumption of a UAV consists of two parts, i.e., communication-related and propulsion power consumption. Here, only the UAV's propulsion power consumption is considered as the communication-related power consumption is usually much smaller than the propulsion power consumption [11]. According to [19], the propulsion power consumption of a fixed-wing UAV with circular and straight trajectories can be modeled as $[c_1 + c_2/(\mathrm{g}^2 r^2)]v^3 + c_2/v$ and $c_1 v^3 + c_2/v$, respectively. Here, $c_1$ and $c_2$ are the parameters depending on the aircraft's weight, wing area, air density, etc., and $g$, $r$, and $v$ denote the acceleration of gravity, the radius of the circular path and the velocity of the UAV, respectively [19]. Then, the optimization problem corresponding to the propulsion energy minimization can be formulated as follows:

$$\begin{aligned} &\left(r_1^*, r_2^*, v_1^*, v_2^*, v_3^*, T_1^*, T_2^*, T_3^*, n^*\right) \\ &= \arg \min_{r_1, r_2, v_1, v_2, v_3, T_1, T_2, T_3, n} T_1 \\ &\left[\left(c_1 + \frac{c_2}{g^2 r_1^2}\right)v_1^3 + \frac{c_2}{v_1}\right] + T_2\left(c_1 v_2^3 + \frac{c_2}{v_2}\right) \\ &\quad + T_3\left[\left(c_1 + \frac{c_2}{g^2 r_2^2}\right)v_3^3 + \frac{c_2}{v_3}\right], \end{aligned} \tag{12a}$$

$$\text{s.t.} \quad r_1 + r_2 \leq L, r_1 > 0, r_2 > 0, \tag{12b}$$

$$V_{\min} \leq v_1, v_2, v_3 \leq V_{\max}, \tag{12c}$$

$$\begin{aligned} T_1 &= \frac{2\pi r_1}{v_1} n, \ (n = 1, 2, \cdots), \\ T_2 &= \frac{L - r_1 - r_2}{v_2}, \\ T_3 &\geq 0, \end{aligned} \tag{12d}$$

$$Q_{\mathrm{R}}(T) \geq Q, Q_{\mathrm{D}}(T) \geq Q, \tag{12e}$$

$$Q_{\mathrm{D}}(t) \leq Q_{\mathrm{R}}(t), 0 \leq t \leq T, \tag{12f}$$

$$T_1 + T_2 + T_3 = T, \tag{12g}$$

where $V_{\min}$ and $V_{\max}$ are the UAV's the minimum and maximum flight velocity constraints, (12b) and (12e) are the practical physical constraints, and (12g) is the mission completion time constraint.

## 4. Solution of the Energy Minimization Problem

In this section, the energy minimization problem (12a)–(12g) is solved, leading to a HCST design. As a first step, the following lemma is presented so as to simplify the optimization problem.

**Lemma 1.** *For problem (12a)–(12g), constraints (12e) and (12f) can be rewritten as follows:*

$$Q_{\mathrm{R}}(T) \geq Q_{\mathrm{D}}(T) = Q. \tag{13}$$

*Proof.* It is noticed that $Q_{\mathrm{R}}(t)$ and $Q_{\mathrm{D}}(t)$ are both monotonically increasing functions for $t \in [0, +\infty$. Moreover, when S and $D$ are located far away, $Q_{\mathrm{R}}(t)$ can be seen as a convex function of $t$, while $Q_{\mathrm{D}}(t)$ is a concave function. Since $Q_{\mathrm{R}}(0) = Q_{\mathrm{D}}(0) = 0$, (12f) can be satisfied if $Q_{\mathrm{R}}(T) \geq Q_{\mathrm{D}}(T)$ holds. Assume that $Q_{\mathrm{D}}(T^*) > Q$ holds, where $T^* = T_1^* + T_2^* + T_3^*$ and $T_1^*$, $T_2^*$, and $T_3^*$ are the solutions of (12a)–(12g). Then, there must exist $\Delta > 0$ such that $T_1^*$, $T_2^*$, and $T_3^* - \Delta$ can satisfy the constraints of (12a)–(12g), and further reduce the power consumption, which contradicts the optimal assumption of $T_1^*$, $T_2^*$, and $T_3^*$. Therefore, the optimal solution of (12a)–(12g) must satisfy $Q_{\mathrm{D}}(T^*) = Q$, and (12e) and (12f) can be rewritten as $Q_{\mathrm{R}}(T) \geq Q_{\mathrm{D}}(T) = Q$.

Denote by $Q_{\mathrm{R}}^{\mathrm{cir1}}$, $Q_{\mathrm{R}}^{\mathrm{str}}$, and $Q_{\mathrm{R}}^{\mathrm{cir2}}$ the sizes of data-bits received by the UAV in the duration of modes 1, 2, and 3, respectively. Denote by $Q_{\mathrm{D}}^{\mathrm{cir1}}$, $Q_{\mathrm{D}}^{\mathrm{str}}$, and $Q_{\mathrm{D}}^{\mathrm{cir2}}$ the sizes of data-bits received by $D$ in the duration of modes 1, 2, and 3, respectively. Then, (13) can be rewritten as follows:

$$Q_{\mathrm{R}}^{\mathrm{cir1}} + Q_{\mathrm{R}}^{\mathrm{str}} + Q_{\mathrm{R}}^{\mathrm{cir2}} \geq Q_{\mathrm{D}}^{\mathrm{cir1}} + Q_{\mathrm{D}}^{\mathrm{str}} + Q_{\mathrm{D}}^{\mathrm{cir2}} = Q, \tag{14}$$

and $Q_{\mathrm{R}}^{\mathrm{cir1}}$ can be expressed as follows:

$$Q_{\mathrm{R}}^{\mathrm{cir1}} = \frac{2n\pi r_1}{v_1}\log_2\left(1 + \frac{P_{\mathrm{S}}\gamma_0}{H^2 + r_1^2}\right). \tag{15}$$

According to [19], $Q_{\mathrm{R}}^{\mathrm{str}}$ can be expressed as follows:

$$Q_{\mathrm{R}}^{\mathrm{str}} = \frac{F_1(L - r_2) - F_1(r_1)}{v_2 \ln 2}, \tag{16}$$

where $F_1(x) = x\ln(1 + P_{\mathrm{S}}\gamma_0/H^2 + x^2) - 2H\tan^{-1}(x/H) + 2\sqrt{H^2 + P_{\mathrm{S}}\gamma_0}\tan^{-1}(x/\sqrt{H^2 + P_{\mathrm{S}}\gamma_0})$.

Since $Q_{\mathrm{R}}^{\mathrm{cir2}}$ is mathematically intractable, a corresponding lower-bound is considered. It should be noted that a lower-bound of $Q_{\mathrm{R}}^{\mathrm{cir2}}$ satisfying (14) can enable (12e) and (12f) to be held. Using inequality (52)in [11], $Q_{\mathrm{R}}^{\mathrm{cir2}}$ can be lower-bounded as follows:

$$\begin{aligned} Q_{\mathrm{R}}^{\mathrm{cir2}} &= \int_{-\pi}^{\frac{v_3}{r_2}T_3 - \pi} \frac{r_2}{v_3}\log_2\left(1 + \frac{P_{\mathrm{S}}\gamma_0}{H^2 + L^2 + 2Lr_2\cos x + r_2^2}\right)dx \\ &\Rightarrow Q_{\mathrm{R}}^{\mathrm{cir2}} \geq T_3\log_2\left(1 + \frac{P_{\mathrm{S}}\gamma_0}{H^2 + L^2 + r_2^2}\right) \\ &\quad - \frac{r_2}{v_3}\frac{2(\log_2 e)P_{\mathrm{S}}\gamma_0 Lr_2}{\left(H^2 + L^2 + r_2^2\right)\left(H^2 + L^2 + r_2^2 + P_{\mathrm{S}}\gamma_0\right)} \\ &\Rightarrow Q_{\mathrm{R}}^{\mathrm{cir2}} \geq T_3 B_1(r_2) + B_2(r_2, v_3) \end{aligned}, \tag{17}$$

where

$$\begin{aligned} B_1(r_2) &= \log_2\left(1 + \frac{P_{\mathrm{S}}\gamma_0}{H^2 + L^2 + r_2^2}\right), \\ B_2(r_2, v_3) &= -\frac{2(\log_2 e)P_{\mathrm{S}}\gamma_0 Lr_2^2}{v_3\left(H^2 + L^2 + r_2^2\right)\left(H^2 + L^2 + r_2^2 + P_{\mathrm{S}}\gamma_0\right)} \end{aligned}. \tag{18}$$

Using the same approach, it is readily to obtain $Q_{\mathrm{D}}^{\mathrm{cir1}} \geq T_1 B_3(r_1) + B_4(r_1, v_1)$, $Q_{\mathrm{D}}^{\mathrm{str}} = F_2(L - r_1) - F_2(r_2)/v_2 \ln 2$ and $Q_{\mathrm{D}}^{\mathrm{cir2}} = T_3\log_2(1 + P_{\mathrm{R}}\gamma_0/H^2 + r_2^2)$, where

$$\begin{aligned} B_3(r_1) &= \log_2\left(1 + \frac{P_{\mathrm{R}}\gamma_0}{H^2 + L^2 + r_1^2}\right) \\ B_4(r_1, v_1) &= \frac{-2\left(\log_2^e\right)P_{\mathrm{R}}\gamma_0 Lr_1^2}{v_1\left(H^2 + L^2 + r_1^2\right)\left(H^2 + L^2 + r_1^2 + P_{\mathrm{R}}\gamma_0\right)} \end{aligned}. \tag{19}$$

And $F_2(x)$ is defined as the following:

$$F_2(x) = x\ln\left(1 + \frac{P_{\mathrm{R}}\gamma_0}{H^2 + x^2}\right) - 2H\tan^{-1}\left(\frac{x}{H}\right) + 2\sqrt{H^2 + P_{\mathrm{R}}\gamma_0}\tan^{-1}\left(\frac{x}{\sqrt{H^2 + P_{\mathrm{R}}\gamma_0}}\right). \tag{20}$$

Since problem (12a)–(12g) is a nonconvex mixed integer programming problem, it cannot be directly solved with standard convex optimization techniques. In the following, problem (12a)–(12g) is divided into three subproblems by solving which a suboptimal solution to the power minimization problem is acquired.

Recall that $S$ and $D$ are located far away and the UAV relay assists the data transfer between $S$ and $D$ by adopting three trajectory modes. In mode 1, the UAV is much closer to S than to $D$, and thus it has a dominant traffic volume in collecting data from $S$. On the contrary, in mode 3 the traffic of the link from $R$ to $D$ is dominant. Therefore, in order to

simplify (12a)–(12g), two subproblems corresponding to the energy minimization in modes 1 and 3 are addressed first, where only the link having the dominant traffic volume is considered. The two subproblems can be formulated as (21a)–(21c) and (22a)–(22c).

$$(\tilde{r}_1, \tilde{v}_1) = \arg\min_{r_1, v_1} T_1 \left[ \left( c_1 r_1 + \frac{c_2}{g^2 r_1} \right) v_1^3 + \frac{c_2 r_1}{v_1} \right], \tag{21a}$$

$$\text{s.t.} Q_{\mathrm{R}}^{\mathrm{cir1}} = T_1 \log_2 \left( 1 + \frac{P_{\mathrm{S}} \gamma_0}{H^2 + r_1^2} \right), \tag{21b}$$

$$v_{\min} \le v_1 \le v_{\max}, 0 < r_1 < L, \tag{21c}$$

$$(\tilde{r}_2, \tilde{v}_3) = \arg\min_{r_2, v_3} T_3 \left[ \left( c_1 + \frac{c_2}{g^2 r_2^2} \right) v_3^3 + \frac{c_2}{v_3} \right], \tag{22a}$$

$$\text{s.t.} Q_{\mathrm{D}}^{\mathrm{cir2}} = T_3 \log_2 \left( 1 + \frac{P_{\mathrm{R}} \gamma_0}{H^2 + r_2^2} \right), \tag{22b}$$

$$v_{\min} \le v_3 \le v_{\max}, 0 < r_2 < L, T_3 \ge 0. \tag{22c}$$

Of note is that in (21a)–(21c) and (22a)–(22c), $Q_{\mathrm{R}}^{\mathrm{cir1}}$ and $Q_{\mathrm{D}}^{\mathrm{cir2}}$ are assumed to be fixed.

For problem (21a)–(21c), substituting (21b) into (21a) leads to

$$(\tilde{r}_1, \tilde{v}_1) = \arg\min_{r_1, v_1} \frac{\left( c_1 + \left( c_2 / g^2 r_1^2 \right) \right) v_1^3 + \left( c_2 / v_1 \right)}{\log_2 \left( 1 + \left( P_{\mathrm{S}} \gamma_0 / \left( H^2 + r_1^2 \right) \right) \right)}, \tag{23a}$$

$$\text{s.t.} v_{\min} \le v_1 \le v_{\max}, 0 < r_1 < L. \tag{23b}$$

It can be found that $[c_1 + c_2/(g^2 r_2^2)] v_1^3 + c_2/v_1$ is a concave function for $v_1 \in (0, +\infty)$. Its extreme point is $v_1 = \{c_2/[3c_1 + 3c_2/(g^2 r_1^2)]\}^{1/4}$. So, the minimum power on the numerator of (23a) can be achieved when the following equation holds:

$$\tilde{v}_1 = \begin{cases} v_{\min}, & \text{if } v_{\min} > \left( \dfrac{c_2 g^2 r_1^2}{3c_1 g^2 r_1^2 + 3c_2} \right)^{1/4}, \\ \left( \dfrac{c_2 g^2 r_1^2}{3c_1 g^2 r_1^2 + 3c_2} \right)^{1/4}, & \text{if } v_{\min} \le \left( \dfrac{c_2 g^2 r_1^2}{3c_1 g^2 r_1^2 + 3c_2} \right)^{1/4} \le v_{\max}, \\ v_{\max}, & \text{if } v_{\max} < \left( \dfrac{c_2 g^2 r_1^2}{3c_1 g^2 r_1^2 + 3c_2} \right)^{1/4}. \end{cases} \tag{24}$$

Substituting (24) into (23a) and then $\tilde{r}_1$ can be obtained by using one-dimensional search over $0 < r_1 < L$.

For problem (22a)–(22c), substituting (22b) into (22a) leads to

$$(\tilde{r}_2, \tilde{v}_3) = \arg\min_{r_2, v_3} \frac{\left( c_1 + \left( c_2 / g^2 r_2^2 \right) \right) v_3^3 + \left( c_2 / v_3 \right)}{\log_2 \left( 1 + \left( P_{\mathrm{R}} \gamma_0 / H^2 + r_2^2 \right) \right)}, \tag{25a}$$

$$\text{s.t.} v_{\min} \le v_3 \le v_{\max}, 0 < r_2 < L. \tag{25b}$$

Likewise, the minimum power on the numerator of (25a) can be achieved when (26) holds.

$$\tilde{v}_3 = \begin{cases} v_{\min}, & \text{if } v_{\min} > \left( \dfrac{c_2 g^2 r_2^2}{3c_1 g^2 r_2^2 + 3c_2} \right)^{1/4}, \\ \left( \dfrac{c_2 g^2 r_2^2}{3c_1 g^2 r_2^2 + 3c_2} \right)^{1/4}, & \text{if } v_{\min} \le \left( \dfrac{c_2 g^2 r_2^2}{3c_1 g^2 r_2^2 + 3c_2} \right)^{1/4} \le v_{\max}, \\ v_{\max}, & \text{if } v_{\max} < \left( \dfrac{c_2 g^2 r_2^2}{3c_1 g^2 r_2^2 + 3c_2} \right)^{1/4}. \end{cases} \tag{26}$$

Substituting (26) into (25a) and then the optimal solution of (25a)–(25b) can be obtained by using one-dimensional search over $0 < r_2 < L$.

Base on the above discussions, (12a)–(12g) can be transformed into

$$\begin{aligned} \left( \tilde{v}_2, \tilde{T}_1, \tilde{T}_3, \tilde{n} \right) = \arg \min_{v_2, T_1, T_3, n} & T_1 \left[ \left( c_1 + \frac{c_2}{g^2 \tilde{r}_1^2} \right) \tilde{v}_1^3 + \frac{c_2}{\tilde{v}_1} \right] \\ & + T_2 \left( c_1 v_2^3 + \frac{c_2}{v_2} \right) + T_3 \left[ \left( c_1 + \frac{c_2}{g^2 \tilde{r}_2^2} \right) \tilde{v}_3^2 + \frac{c_2}{\tilde{v}_3^2} \right], \end{aligned} \tag{27a}$$

$$\text{s.t.} V_{\min} \le v_2 \le V_{\max}, \tag{27b}$$

$$\begin{aligned} T_1 &= \frac{2\pi \tilde{r}_1}{\tilde{v}_1} n, \ (n = 1, 2, \cdots), \\ T_2 &= \frac{L - \tilde{r}_1 - \tilde{r}_2}{v_2}, T_3 \ge 0, \end{aligned} \tag{27c}$$

$$Q_{\mathrm{R}}^{\mathrm{cir1}} + Q_{\mathrm{R}}^{\mathrm{str}} + B_1 (\tilde{r}_2) T_3 + B_2 (\tilde{r}_2, \tilde{v}_3) \ge Q, \tag{27d}$$

$$B_3 (\tilde{r}_1) T_1 + B_4 (\tilde{r}_1, \tilde{v}_1) + Q_{\mathrm{D}}^{\mathrm{str}} + Q_{\mathrm{D}}^{\mathrm{cir2}} = Q. \tag{27e}$$

In (27a)–(27e), $\tilde{r}_1$ and $\tilde{v}_1$ are the optimal solutions of (21a)–(21c), and $\tilde{r}_2$ and $\tilde{v}_3$ are the optimal solutions of (22a)–(22c).

However, (27a)–(27e) is still hard to solve due to the integer constraint $n$. Then, the following two lemmas are proposed so as to simplify problem (27a)–(27e).

**Lemma 2.** *For problem (27a)–(27e), the optimal solution of the number of the laps in mode 1 can be given by*

$$\tilde{n} \in \left\{ \left\lceil \frac{\hat{T}_1 \tilde{v}_1}{2\pi \tilde{r}_1} \right\rceil, \left\lceil \frac{\hat{T}_1 \tilde{v}_1}{2\pi \tilde{r}_1} \right\rceil \right\}, \tag{28}$$

*where $\tilde{r}_1$ and $\tilde{v}_1$ are the optimal solutions of (21a)–(21c), and $\hat{T}_1$ is given by (A.3) in Appendix A.*

*Proof.* See Appendix A.

**Lemma 3.** *Denote by $\tilde{Q}_{\mathrm{R}}^{\mathrm{cir1}}$ and $\tilde{Q}_{\mathrm{R}}^{\mathrm{str}}$ the optimal data-bits received by R in modes 1 and 2, respectively, which can be obtained by solving problem (27a)–(27e) and then substituting the obtained solutions into (15) and (16). Let $\hat{Q}_{\mathrm{R}}^{\mathrm{cir1}} = Q - \tilde{Q}_{\mathrm{R}}^{\mathrm{str}} - B_1(\tilde{r}_2)\tilde{T}_3 - B_2(\tilde{r}_2, \tilde{v}_3)$. Then, $\tilde{Q}_{\mathrm{R}}^{\mathrm{cir1}}$ can be expressed as follows:*

$$\tilde{Q}_{\mathrm{R}}^{\mathrm{cir1}} = \max\left\{ \hat{Q}_{\mathrm{R}}^{\mathrm{cir1}}, Q_{\mathrm{ext}} \right\}, \tag{29}$$

*where*
$Q_{\mathrm{ext}} = 2n\pi\sqrt{\tilde{r}_1}\,(3c_2 + 3c_1 g^2 \tilde{r}_1^2 / c_2 g^2)^{1/4} \log_2\,(1 + P_{\mathrm{S}}\gamma_0 / H^2 + \tilde{r}_1^2)$.

*Proof.* By fixing the value of the radius and the speed in mode 1, it can be easily found that the system energy consumption of the UAV is monotonically decreasing for $Q_{\mathrm{R}}^{\mathrm{cir1}} \in (0, Q_{\mathrm{ext}})$ and monotonically increasing for $Q_{\mathrm{R}}^{\mathrm{cir1}} \in (Q_{\mathrm{ext}}, +\infty)$. Since $B_1(\tilde{r}_2)\tilde{T}_3 + B_2(\tilde{r}_2, \tilde{v}_3)$ is a lower-bound of data-bits received by the UAV in mode 3, $\tilde{Q}_{\mathrm{R}}^{\mathrm{cir1}} \geq \hat{Q}_{\mathrm{R}}^{\mathrm{cir1}}$ must hold. In the following, two cases, i.e., $\hat{Q}_{\mathrm{R}}^{\mathrm{cir1}} \geq Q_{\mathrm{ext}}$ and $\hat{Q}_{\mathrm{R}}^{\mathrm{cir1}} < Q_{\mathrm{ext}}$, are considered. For the case where $\hat{Q}_{\mathrm{R}}^{\mathrm{cir1}} \geq Q_{\mathrm{ext}}$, if $\tilde{Q}_{\mathrm{R}}^{\mathrm{cir1}} - \hat{Q}_{\mathrm{R}}^{\mathrm{cir1}} > 0$, we can always find a smaller system energy consumption by reducing the energy consumption of mode 1, while fixing the energy consumption of modes 2 and 3. It contradicts the optimal assumption, and thus $\tilde{Q}_{\mathrm{R}}^{\mathrm{cir1}} = \hat{Q}_{\mathrm{R}}^{\mathrm{cir1}}$ must hold in this situation. For the case where $\hat{Q}_{\mathrm{R}}^{\mathrm{cir1}} < Q_{\mathrm{ext}}$, if $|\tilde{Q}_{\mathrm{R}}^{\mathrm{cir1}} - Q_{\mathrm{ext}}| > 0$, we can always find a smaller system energy consumption by reducing the energy consumption of mode 1 while fixing the power consumption of modes 2 and 3. It also contradicts the optimal assumption, and thus $\tilde{Q}_{\mathrm{R}}^{\mathrm{cir1}} = Q_{\mathrm{ext}}$ must hold. In conclusion, $\tilde{Q}_{\mathrm{R}}^{\mathrm{cir1}} = \max\left\{ \hat{Q}_{\mathrm{R}}^{\mathrm{cir1}}, Q_{\mathrm{ext}} \right\}$ holds.

For the case that $\tilde{n}$ is known, problem (27a)–(27e) can be rewritten as (30a)–(30d).

$$\left(\tilde{v}_2, \tilde{T}_3\right) = \underset{v_2, T_3}{\arg\min}\ \frac{2\pi\tilde{r}_1}{\tilde{v}_1}\tilde{n}\left[\left(c_1 + \frac{c_2}{g^2\tilde{r}_1^2}\right)\tilde{v}_1^3 + \frac{c_2}{\tilde{v}_1}\right] + \frac{L - \tilde{r}_1 - \tilde{r}_2}{v_2}\left(c_1 v_2^3 + \frac{c_2}{v_2}\right) + T_3\left[\left(c_1 + \frac{c_2}{g^2\tilde{r}_2^2}\right)\tilde{v}_3^2 + \frac{c_2}{\tilde{v}_3^2}\right], \tag{30a}$$

$$\text{s.t.} V_{\min} \leq v_2 \leq V_{\max}, T_3 \geq 0, \tag{30b}$$

$$\frac{2\tilde{n}\pi\tilde{r}_1}{\tilde{v}_1}\log_2\left(1 + \frac{P_{\mathrm{S}}\gamma_0}{H^2 + \tilde{r}_1^2}\right) + B_1(\tilde{r}_2)T_3 + B_2(\tilde{r}_2, \tilde{v}_3) + \frac{F_1(L - \tilde{r}_2) - F_1(\tilde{r}_1)}{v_2 \ln 2} \geq Q, \tag{30c}$$

$$B_3(\tilde{r}_1)\tilde{T}_1 + B_4(\tilde{r}_1, \tilde{v}_1) + \frac{F_2(L - \tilde{r}_1) - F_2(\tilde{r}_2)}{v_2 \ln 2} + T_3\log_2\left(1 + \frac{P_{\mathrm{R}}\gamma_0}{H^2 + \tilde{r}_2^2}\right) = Q, \tag{30d}$$

in (30a)–(30d), $\tilde{T}_1$ can be achieved by substituting $\tilde{r}_1$, $\tilde{v}_1$, and $\tilde{n}$ into (1). It can be observed that the cost function and the constraint set in (30a)–(30d) are convex, and thus it is a convex optimization problem. By solving the Karush-Kuhn-Tucker (KKT) equations, the solution of (30a)–(30d) can be acquired, giving

(1) Initialize $Q_R^{cir1} = Q$, $n = N$ ($N$ is a large integer), tolerance $\varepsilon > 0$.
(2) Solve problem (25a)-(25b) and the value of $\tilde{r}_2$ and $\tilde{v}_3$ can be achieved.
(3) **repeat**
(4) Substitute $Q_R^{cir1}$ and $n$ into problem (23a)-(23b). Then update the value of $\tilde{r}_1$ and $\tilde{v}_1$.
(5) According to (31) and (32), $\tilde{v}_2$ and $\tilde{T}_3$ can be achieved. Then according Lemma 3, the value of $\tilde{Q}_R^{cir1}$ can be achieved. Let $\Delta Q = |\tilde{Q}_R^{cir1} - Q_R^{cir1}|$.
(6) Update $Q_R^{cir1} = \tilde{Q}_R^{cir1}$.
(7) **until** $\Delta Q \le \varepsilon$.
(8) Output the sub-optimal radius $\tilde{r}_1$, velocity $\tilde{v}_1$ and duration $\tilde{T}_1$ in mode 1; output the sub-optimal velocity $\tilde{v}_2$ and duration $\tilde{T}_2$ in mode 2; output the suboptimal duration $\tilde{T}_3$ in mode 3 and calculate the total energy consumption $E$.

Algorithm 1: Iteration algorithm for solving the propulsion energy minimization problem.

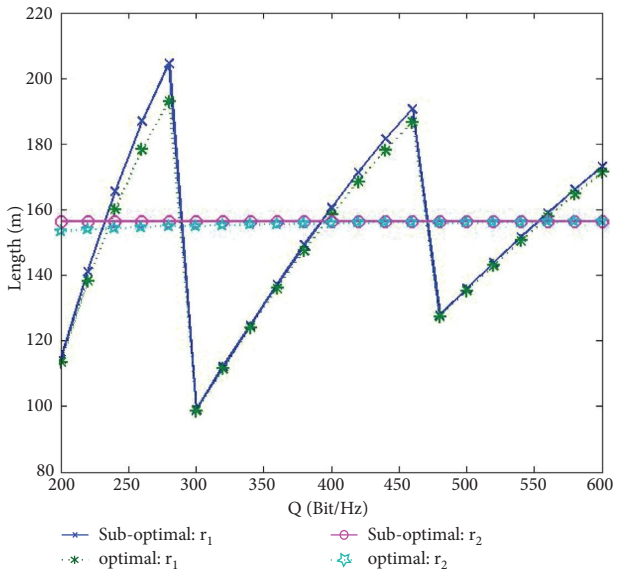


Figure 2: The circular radius of the UAV in modes 1 and 3 versus the total data-bits ($Q$).

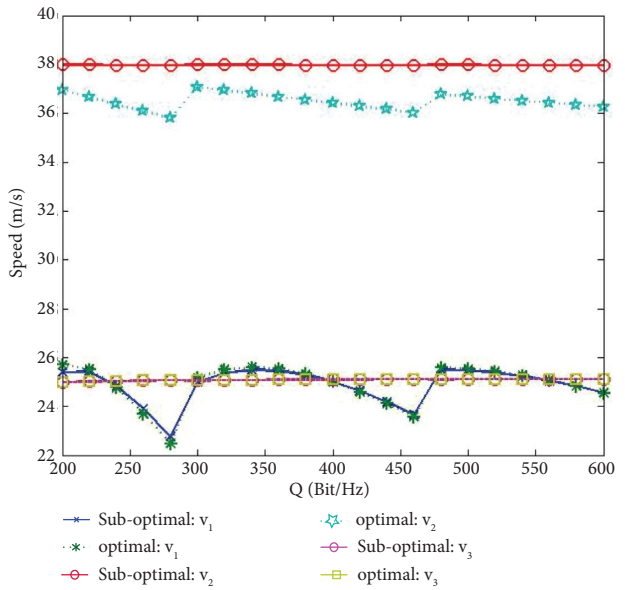


Figure 3: The flight velocity of the UAV versus the total data-bits ($Q$).

$$\tilde{v}_2 = -0.5\sqrt{f_2} + 0.5\sqrt{-f_2 + \frac{a_9 a_{10}}{c_1 a_5 \sqrt{f_2}(L - \tilde{r}_1 - \tilde{r}_2)}}, \tag{31}$$

$$\tilde{T}_3 = \frac{2f_2 k a_{10} - 4a_9 a_{10}^2 \tilde{v}_2 - 2\sqrt{f_2}\left[a_{10}(2a_9 a_{10} - k\tilde{v}_2) - 8c_2 a_5 (L - \tilde{r}_1 - \tilde{r}_2)\left(a_8 - b_3 \tilde{T}_1\right)\right]}{16 c_2 a_5^2 \sqrt{f_2}(L - \tilde{r}_1 - \tilde{r}_2)} + \frac{4c_1 a_5 a_{10}\left[f_2 k - 24 c_2 a_5 (L - \tilde{r}_1 - \tilde{r}_2)\right]\left(\sqrt{f_2} + \tilde{v}_2\right)}{16 c_2 a_5^2 k}, \tag{32}$$

where $k = \left\{3\sqrt{3}\sqrt{c_1^2 a_5^2 (L - \tilde{r}_1 - \tilde{r}_2)^2 c_1^2 [27 a_9^4 a_{10}^4 + 4096 c_1 c_2^3 a_5^4 (L - \tilde{r}_1 - \tilde{r}_2)^4]} - 27 c_1 a_9^2 a_5 a_{10}^2 (L - \tilde{r}_1 - \tilde{r}_2)\right\}^{1/3}$, $f_2 = 8c_2 a_5 (L - \tilde{r}_1 - \tilde{r}_2)/k - k/6c_1 a_5 (L - \tilde{r}_1 - \tilde{r}_2)$, $a_5 = \log_2(1 + P_R \gamma_0 / H^2 + \tilde{r}_2^2)$, $a_9 = (c_1 + c_2/g^2 \tilde{r}_2^2)\tilde{v}_3^2 + c_2/\tilde{v}_3^2$, and $a_{10} = F_2(L - \tilde{r}_1) - F_2(\tilde{r}_2)/\ln 2$.

According to Lemma 2 and Lemma 3, an iterative algorithm is proposed to solve problem (28), leading to a suboptimal solution to the propulsion energy minimization problem (12a)–(12g). First, $\tilde{r}_1$, $\tilde{v}_1$, $\tilde{r}_2$, and $\tilde{v}_3$ are acquired by solving (23a)-(23b) and (25a)-(25b) with fixed $Q_R^{cir1}$ and $Q_D^{cir2}$. Second, substituting $\tilde{r}_1$, $\tilde{v}_1$, $\tilde{r}_2$, and $\tilde{v}_3$ into (29) and then according to Lemma 3, $\tilde{Q}_R^{cir1}$ can be achieved. Next, set $Q_R^{cir1} = \tilde{Q}_R^{cir1}$ and repeat the first two steps until a convergent solution is found. Then, the algorithm of achieving the suboptimal solution of the propulsion energy minimization problem can be given in Algorithm 1.

Table 1: The number of laps in mode 1 versus the total data-bits $Q$.

| $Q$ (bit) | $n$ (laps) |
|---|---|
| 200 | 1 |
| 220 | 1 |
| 240 | 1 |
| 260 | 1 |
| 280 | 1 |
| 300 | 2 |
| 320 | 2 |
| 340 | 2 |
| 360 | 2 |
| 380 | 2 |
| 400 | 2 |
| 420 | 2 |
| 440 | 2 |
| 460 | 2 |
| 480 | 3 |
| 500 | 3 |
| 520 | 3 |
| 540 | 3 |
| 560 | 3 |
| 580 | 3 |
| 600 | 3 |

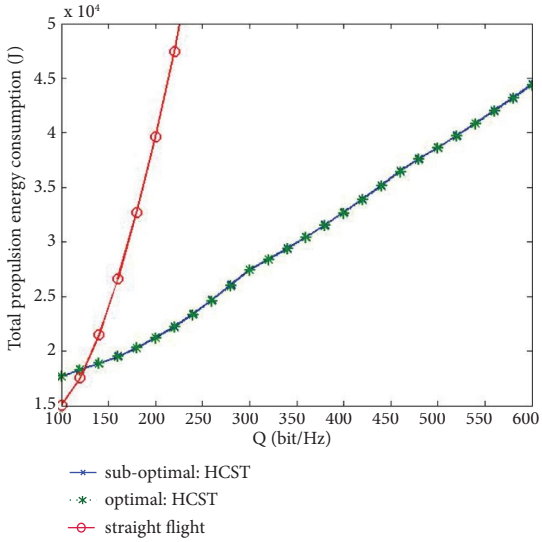


Figure 4: Total propulsion energy consumption versus the total data-bits ($Q$).

It is worth-mentioning that according to Lemma 2, $\tilde{n}$ has two possible solutions, i.e., $\lfloor \widehat{T}_1 \tilde{v}_1 / 2\pi \tilde{r}_1 \rfloor$ and $\lceil \widetilde{T}_1 \tilde{v}_1 / 2\pi \tilde{r}_1 \rceil$. Therefore, two sets of solution could be achieved if substituting $\tilde{n} = \lfloor \widehat{T}_1 \tilde{v}_1 / 2\pi \tilde{r}_1 \rfloor$ and $\tilde{n} = \lceil \widetilde{T}_1 \tilde{v}_1 / 2\pi \tilde{r}_1 \rceil$ into the iteration algorithm. Actually, the final solution of the algorithm is the one having the smaller energy consumption.

## 5. Simulation Results and Discussion

In this section, computer simulations are conducted to validate the proposed HCST design. In order to make comparisons, the energy consumption of straight and circular flight trajectories are included. In Appendix B, a brief description is given to explain how the solutions of the system energy consumption are obtained for the straight and circular flight trajectories. Here, the UAV altitude is fixed at $H = 200m$. The noise power is set to $-110$ dB m and the reference channel power is set to $\beta_0 = -50$ dB. Furthermore, $c_1 = 9.26 \times 10^{-4}$, $c_2 = 2250$, $V_{\min} = 10$m/s and $V_{\max} = 50$m/s are assumed.

Figures 2 and 3 give the solutions of the circular radius and the speed of the UAV relay in different modes, where the corresponding number of laps that $R$ flies in mode 1 is listed in Table 1. It should be noted that the suboptimal solutions are achieved by carrying out the proposed iteration algorithm. While the optimal solution is obtained by conducting a brute search algorithm. Here, the distance between S and $D$ is set to $L = 5000$m, the transmit power of S and $R$ is set to $P_S = P_R = 1$W. It is shown in Figures 2 and 3 that the curves corresponding to the suboptimal and optimal solutions are quite close to each other, confirming the effectiveness of the proposed iteration algorithm. In addition, Figures 2 and 3 show that the circular radius $r_1$ is monotonically increasing for $Q \in (200, 280)$ while the speed $v_1$ is monotonically decreasing for $Q \in (200, 280)$. According to Table 1, the UAV relay only flies one lap for $Q \in (200, 280)$. In order for the UAV relay receives more data-bits, larger $r_1$ and lower $v_1$ are needed. For $Q \in (280, 300)$, there exists a jump phenomenon regarding the circular radius $r_1$ and the speed $v_1$, namely, the values of $r_1$ and $v_1$ decrease rapidly as shown in Figures 2 and 3. According to Table 1, it can be seen that the number of laps that the UAV relay flies in mode 1 increases form 1 to 2 when $Q$ increases from 280 to 300. Since the UAV relay flies more laps in mode 1, less values of $r_1$ and $v_1$ are needed to obtain longer flight duration. The UAV relay can then receive more data-bits accordingly. Furthermore, it can be observed that the circular radius $r_2$ and the speed $v_3$ are almost not changed. This is because no flight-lap constraint exists in mode 3, and the corresponding optimal solutions are achieved by considering only the dominant-traffic-link from $R$ to $D$.

Figures 4 and 5 plot the total energy consumption versus the total data-bits $Q$ and the distance $L$. Here, the HCST and the conventional straight and circular flight trajectories are included. In Figures 4 and 5, the transmit power of $S$ and $R$ is set to $P_S = P_R = 1$W. In Figure 4, the distance between $S$ and $D$ is set to $L = 5000$. Figure 4 illustrates that the HCST can save more energy compare with the straight flight trajectory when the total data-bits $Q$ is large. For instance, the HCST can achieve about 18.4 kW energy saving compared with the straight flight trajectory when $Q = 200$bits. In Figure 5, the total data-bit is set to $Q = 300$. Figure 5 shows that the HCST can save more energy compare with the circular flight trajectory when the distance $L$ is large. For instance, the HCST can achieve about 2.7 kW energy saving compared with the circular flight trajectory when $L = 1000$. In summary, the HCST performs extremely well for long distance and big data communication cases compared with the conventional straight and circular trajectories.

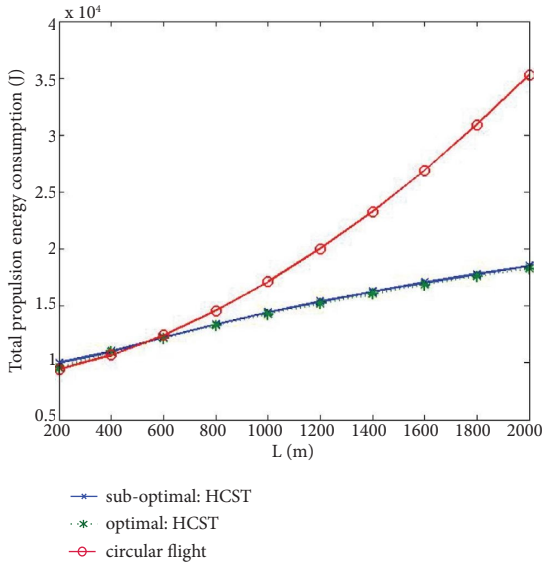


Figure 5: Total propulsion energy consumption the distance ($L$).

## 6. Conclusions

This paper investigates an optimization problem corresponding to the propulsion energy minimization of a fixed-wing-UAV-assisted mobile relaying system subject to the total data-bit constraint. In order to solve the optimization problem, an iteration algorithm is proposed to achieve a suboptimal solution, which leads to a new HCST design with three flying modes. Simulation results demonstrated that the HCST design performs better than the conventional straight or circular flight trajectory in terms of energy saving, especially for the case that the source and the destination locate far away and desire to transfer big data-bits between them.

## Appendix

### A

For problems (27a)–(27e), it is readily to find that the total propulsion energy consumption is monotonically decreasing at first and then monotonically increasing when $n$ increases from 0 to infinity. Firstly, we ignore the constraint that $n$ should be an integer. Then, the suboptimal trajectories of modes 1 and 3 can be derived by solving problems (23a)-(23b) and (25a)-(25b). Then, problem (27a)–(27e) can be rewritten as follows:

$$\widehat{T}_1 = \arg\min_{T_1} T_1\left[\left(c_1 + \frac{c_2}{g^2\widetilde{r}_1^2}\right)\widetilde{v}_1^2 + \frac{c_2}{\widetilde{v}_1^2}\right] + \frac{L - \widetilde{r}_1 - \widetilde{r}_2}{v_2}\left(c_1 v_2^3 + \frac{c_2}{v_2}\right) + T_3\left[\left(c_1 + \frac{c_2}{g^2\widetilde{r}_2^2}\right)\widetilde{v}_3^2 + \frac{c_2}{\widetilde{v}_3^2}\right], \tag{A.1a}$$

$$\text{s.t.} V_{\min} \le v_2 \le V_{\max}, \tag{A.1b}$$

$$T_1 \ge 0, T_3 \ge 0, \tag{A.1c}$$

$$Q_{\mathrm{R}}^{\mathrm{cir1}} + Q_{\mathrm{R}}^{\mathrm{str}} + B_1(\widetilde{r}_2)T_3 + B_2(\widetilde{r}_2, \widetilde{v}_3) \ge Q, \tag{A.1d}$$

$$B_3(\widetilde{r}_1)T_1 + B_4(\widetilde{r}_1, \widetilde{v}_1) + Q_{\mathrm{D}}^{\mathrm{str}} + Q_{\mathrm{D}}^{\mathrm{cir2}} = Q. \tag{A.1e}$$

Since problem (A.1a)–(A.1e) is a convex optimization problem, it can be solved by solving the KKT equations, and the optimal value of $\widetilde{n}$ can be given as follows:

$$\widetilde{n} = \frac{\widehat{T}_1 \widetilde{v}_1}{2\pi\widetilde{r}_1}, \tag{A.2}$$

where

$$\tilde{T}_1 = \frac{\left\{-192\times 2^{1/3}a_2^2(a_4a_5-a_6b_1)(a_3a_5-b_1b_3)^2c_1c_2\sqrt{f_1}\left(\sqrt{f_1}+v_2\right)+2(a_4a_5-a_6b_1)k_1\left(\sqrt{f_1}+v_2\right)\times\left[-4(a_9a_3a_6+a_1a_4a_5-a_1a_6b_1-a_9a_4b_3)+2^{2/3}\sqrt{f_1}k_1+8a_2(a_3a_5-b_1b_3)\sqrt{f_1}k_1[4a_5a_7c_2+a_4a_5c_1f_1\left(\sqrt{f_1}+v_2\right)\right]-4b_1a_6c_2-a_6b_1c_1f_1\left(\sqrt{f_1}+v_2\right)]\right\}}{\left[32a_2(a_3a_5-b_1b_3)^2c_2\sqrt{f_1}k_1\right]}. \tag{A.3}$$

$$\begin{aligned}
v_2 &= \frac{1}{2}\times\sqrt{a_1(a_4a_5+a_3a_6-a_6b_1-a_4b_3)/\left[a_2(a_3a_5-b_1b_3)c_1\sqrt{f_1}\right]-f_1}-\frac{1}{2}\times\sqrt{f_1},\\
f_1 &= \frac{\left[96a_2^2(a_3a_5-b_1b_3)^2c_1c_2-2^{1/3}k^2\right]}{\left[6\times 2^{2/3}a_2c_1k(a_3a_5-b_1b_3)\right]},\\
k &= \left\{6\sqrt{3}\sqrt{a_2^2(a_3a_5-b_1b_3)^2c_1^2\left[27a_1^4(a_3a_6+a_4a_5-a_6b_1-a_4b_3)^4+4096a_2^4(a_3a_5-b_1b_3)^4c_1c_2^3\right]}\right.\\
&\quad \left.-54a_1^2a_2(a_3a_6+a_4a_5-a_6b_1-a_4b_3)^2(a_3a_5-b_1b_3)c_1\right\}^{1/3},\\
a_1 &= \left(c_1+\frac{c_2}{g^2\tilde{r}_1^2}\right)\tilde{v}_1^2+\frac{c_2}{\tilde{v}_1^2},\\
a_2 &= L-\tilde{r}_1-\tilde{r}_2,\\
a_3 &= \log_2\left(1+\frac{P_S\gamma_0}{H^2+\tilde{r}_1^2}\right),\\
a_4 &= \frac{F_1(L-\tilde{r}_2)-F_1(\tilde{r}_1)}{\ln 2},\\
a_5 &= \log_2\left(1+\frac{P_R\gamma_0}{H^2+\tilde{r}_2^2}\right),\\
a_6 &= \frac{F_2(L-\tilde{r}_1)-F_2(\tilde{r}_2)}{\ln 2},\\
a_7 &= Q-b_2,\\
a_8 &= Q-b_4,\\
a_9 &= \left(c_1+\frac{c_2}{g^2\tilde{r}_2^2}\right)\tilde{v}_3^2+\frac{c_2}{\tilde{v}_3^2},
\end{aligned} \tag{A.4}$$

where $b_1 = B_1(\tilde{r}_2)$, $b_2 = B_2(\tilde{r}_2,\tilde{v}_2)$, $b_3 = B_3(\tilde{r}_1)$ and $b_4 = B_4(\tilde{r}_1,\tilde{v}_1)$. Recall that the UAV has to fly the whole laps in mode 1, namely, $\tilde{n}$ should be an integer, the optimal laps in mode 1 shall be $\lfloor \tilde{T}_1\tilde{v}_1/2\pi\tilde{r}_1 \rfloor$ or $\lceil \tilde{T}_1\tilde{v}_1/2\pi\tilde{r}_1 \rceil$.

## B

For the case that the UAV relay flies from $(r_1, 0, H)$ to $(L, 0, H)$ along a straight path, i.e., the straight flight trajectory case, the optimization problem corresponding to the propulsion energy minimization can be written as follows:

$$(r_2^*, v_2^*) = \arg\min_{r_2,v_2} \frac{L-r_2}{v_2}\left(c_1v_2^3+\frac{c_2}{v_2}\right), \tag{B.1a}$$

$$\text{s.t.}\frac{F_1(L-r_2)-F_1(0)}{v_2\ln 2} \geq Q, \tag{B.1b}$$

$$\frac{F_2(L)-F_2(r_2)}{v_2\ln 2} = Q, \tag{B.1c}$$

where $F_1(x) = x\ln(1+P_S\gamma_0/H^2+x^2) - 2H\tan^{-1}(x/H) + 2\sqrt{H^2+P_S\gamma_0}\tan^{-1}(x/\sqrt{H^2+P_S\gamma_0})$ and $F_2(x) = x\ln(1+P_R\gamma_0/H^2+x^2) - 2H\tan^{-1}(x/H) + 2\sqrt{H^2+P_R\gamma_0}\tan^{-1}(x/\sqrt{H^2+P_R\gamma_0})$.

Problem (B.1a)–(B.1c) can be solved by using the fmincon function from the Matlab optimization toolbox.

For the case that the UAV relay flies along a circular path with a center at $(L/2, 0, H)$, and with radius $r$ and speed $v$, i.e., the circular flight trajectory case, the optimization problem corresponding to the propulsion energy minimization can be written as follows:

$$(r^*, v^*) = \arg\min_{r,v} T\left[\left(c_1+\frac{c_2}{g^2r^2}\right)v^3+\frac{c_2}{v}\right], \tag{B.2a}$$

$$\text{s.t.}Q_R(T) \geq Q, Q_D(T) \geq Q. \tag{B.2b}$$

Using inequality (52) in [11], the lower-bounds of $Q_R(T)$ and $Q_D(T)$ can be written as (B.3) and (B.4).

$$Q_{\mathrm{D}}(T) \geq T \log_2\left(1+\frac{P_{\mathrm{R}}\gamma_0}{H^2+1/4L^2+r^2}\right)-\frac{r}{v}\frac{(\log_2 e)P_{\mathrm{R}}\gamma_0 Lr}{\left(H^2+1/4L^2+r^2\right)\left(H^2+1/4L^2+r^2+P_{\mathrm{R}}\gamma_0\right)}, \tag{B.3}$$

$$Q_{\mathrm{R}}(T) \geq T \log_2\left(1+\frac{P_{\mathrm{S}}\gamma_0}{H^2+1/4L^2+r^2}\right)-\frac{r}{v}\frac{(\log_2 e)P_{\mathrm{S}}\gamma_0 Lr}{\left(H^2+1/4L^2+r^2\right)\left(H^2+1/4L^2+r^2+P_{\mathrm{S}}\gamma_0\right)}. \tag{B.4}$$

Then, substituting the lower-bounds given in (B.3) and (B.4) into (B.2b) and using the Matlab fmincon function, problem (B.2a)-(B.2b) can be solved, leading to the corresponding minimum propulsion energy.

## Data Availability

Data sharing is not applicable to this article as no datasets were generated or analysed during the current study.

## Disclosure

This work is an updated version of our previously completed preprint [23] which can be reached by the link: "https://assets.researchsquare.com/files/rs-915825/v1.covered.pdf?c=1632937413."

## Conflicts of Interest

The authors declare that there are no conflicts of interest regarding the publication of this paper.

## Acknowledgments

This work was supported in part by the Innovation Training Program for College Students (Grant no. 202210304031Z), by the National Natural Science Foundation of China (Grant no. 61871241), and by the Science and Technology Program of Nantong (Grant no. JC2019114).

## References

[1] Z. Yao, W. Cheng, W. Zhang, and H. Zhang, "Resource allocation for 5G-UAV-based emergency wireless communications," *IEEE Journal on Selected Areas in Communications*, vol. 39, no. 11, pp. 3395–3410, 2021.

[2] Q. Song, Y. Zeng, J. Xu, and S. Jin, "A survey of prototype and experiment for UAV communications," *Science China Information Sciences*, vol. 64, no. 4, pp. 140301–140321, 2021.

[3] M. Hua, Y. Wang, C. Li, Y. Huang, and L. Yang, "Energy-efficient optimization for UAV-aided cellular offloading," *IEEE Wireless Communications Letters*, vol. 8, no. 3, pp. 769–772, 2019.

[4] M. A. Ali, Y. Zeng, and A. Jamalipour, "Software-defined coexisting UAV and WiFi: delay-oriented traffic offloading and UAV placement," *IEEE Journal on Selected Areas in Communications*, vol. 38, no. 6, pp. 988–998, 2020.

[5] S. Zhang, J. Zhou, D. Tian, Z. Sheng, X. Duan, and V. CM. Leung, "Robust cooperative communication optimization for multi-UAV-aided vehicular networks," *IEEE Wireless Communications Letters*, vol. 10, no. 4, pp. 780–784, 2021.

[6] S. K. Singh, K. Agrawal, K. Singh, CP. Li, and WJ. Huang, "On UAV selection and position-based throughput maximization in multi-UAV relaying networks," *IEEE Access*, vol. 8, pp. 144039–144050, 2020.

[7] J. Miao and Z. Zheng, "Cooperative jamming for secure UAV-enabled mobile relay system," *IEEE Access*, vol. 8, pp. 48943–48957, 2020.

[8] W. Shi, Y. Sun, M. Liu et al., "Joint UL/DL resource allocation for UAV-aided full-duplex NOMA communications," *IEEE Transactions on Communications*, vol. 69, no. 12, pp. 8474–8487, 2021.

[9] J. Gu, H. Wang, G. Ding, Y. Xu, Z. Xue, and H. Zhou, "Energy-constrained completion time minimization in UAV-enabled internet of things," *IEEE Internet of Things Journal*, vol. 7, no. 6, pp. 5491–5503, 2020.

[10] Y. Wang, Z. Gao, J. Zhang et al., "Trajectory design for UAV-based internet of things data collection: a deep reinforcement learning approach," *IEEE Internet of Things Journal*, vol. 9, no. 5, pp. 3899–3912, 2022.

[11] Y. Zeng and R. Zhang, "Energy-efficient UAV communication with trajectory optimization," *IEEE Transactions on Wireless Communications*, vol. 16, no. 6, pp. 3747–3760, 2017.

[12] Y. Zeng, R. Zhang, and T. J. Lim, "Throughput maximization for UAV-enabled mobile relaying systems," *IEEE Transactions on Communications*, vol. 64, no. 12, pp. 4983–4996, 2016.

[13] J. Fan, M. Cui, G. Zhang, and Y. Chen, "Throughput improvement for multi-hop UAV relaying," *IEEE Access*, vol. 7, pp. 147732–147742, 2019.

[14] J.-H. Lee, K.-H. Park, Y.-C. Ko, and M.-S. Alouini, "Throughput maximization of mixed FSO/RF UAV-aided mobile relaying with a buffer," *IEEE Transactions on Wireless Communications*, vol. 20, no. 1, pp. 683–694, 2021.

[15] Q. Chen, "Joint position and resource optimization for multi-UAV-aided relaying systems," *IEEE Access*, vol. 8, pp. 10403–10415, 2020.

[16] B. Li, S. Zhao, R. Zhang, and L. Yang, "Full-duplex UAV relaying for multiple user pairs," *IEEE Internet of Things Journal*, vol. 8, no. 6, pp. 4657–4667, 2021.

[17] D. H. Choi, S. H. Kim, and D. K. Sung, "Energy-efficient maneuvering and communication of a single UAV-based relay," *IEEE Transactions on Aerospace and Electronic Systems*, vol. 50, no. 3, pp. 2320–2327, 2014.

[18] G. Zhang, X. Ou, M. Cui, Q. Wu, S. Ma, and W. Chen, "Cooperative UAV enabled relaying systems: joint trajectory and transmit power optimization," *IEEE Transactions on Green Communications and Networking*, vol. 6, no. 1, pp. 543–557, 2022.

[19] D. C. Yang, Q. Q. Wu, Y. Zeng, and R. Zhang, "Energy tradeoff in ground-to-UAV communication via trajectory design," *IEEE Transactions on Vehicular Technology*, vol. 67, no. 7, pp. 6721–6726, 2018.

[20] N. Qi, M. Wang, W. J. Wang, TA. Tsiftsis, R. Yao, and G. Yang, "Energy efficient full-duplex UAV relaying networks under load carry and delivery scheme," *IEEE Access*, vol. 8, no. 8, pp. 74349–74358, 2020.

[21] Y. Zeng, J. Xu, and R. Zhang, "Energy minimization for wireless communication with rotary-wing UAV," *IEEE Transactions on Wireless Communications*, vol. 18, no. 4, pp. 2329–2345, 2019.

[22] T. Zhang, G. Liu, H. Zhang, W. Kang, GK. Karagiannidis, and A. Nallanathan, "Energy-efficient resource allocation and trajectory design for UAV relaying systems," *IEEE Transactions on Communications*, vol. 68, no. 10, pp. 6483–6498, 2020.

[23] X. Ji, T. Wang, C. Qian, and C. Huang, "Propulsion energy minimization for fixed-wing-UAV-assisted full-duplex mobile relaying via hybrid trajectory design," 2021, https://assets.researchsquare.com/files/rs-915825/v1.covered.pdf?c=1632937413.